Am J Transl Res 2022;14(5):3052-3065
www.ajtr.org /ISSN:1943-8141/AJTR0141665

Original Article

Integrated analysis reveals prognostic value and mesenchymal identity suppression by glycoprotein M6B in glioma

Zong Miao[1*], Liangyuan Geng[1*], Lei Xu[1], Yangfan Ye[1], Chao Wu[3], Wei Tian[2,1], Ning Liu[1]

[1]*Department of Neurosurgery, The First Affiliated Hospital of Nanjing Medical University, Nanjing, Jiangsu, China;* [2]*Department of Neurosurgery, Affiliated Hospital of Jiangnan University, Wuxi, Jiangsu, China;* [3]*Nantong University, Nantong, Jiangsu, China.* [*]*Equal contributors.*

Received January 10, 2022; Accepted April 26, 2022; Epub May 15, 2022; Published May 30, 2022

Abstract: Glioblastoma (GBM) stem cells (GSCs) possess multilineage differentiation potential, which is responsible for cancer progression. Glycoprotein M6B (GPM6B) is a pivotal enzyme in regulating intracranial cell differentiation and neuronal myelination, and is widely studied in several cancers. However, research on GPM6B in glioma is limited. In this study, we analyzed the clinical and molecular characteristics of GPM6B using RNA sequencing data of glioma samples from the Chinese Glioma Genome Atlas (CGGA) and The Cancer Genome Atlas (TCGA) datasets. Quantitative real-time PCR (qRT-PCR), western blot (WB), and immunohistochemistry (IHC) were performed for further validation. Moreover, a neurosphere formation assay, extreme limiting dilution assay, and bioluminescent imaging were employed to validate the therapeutic effects targeted on GPM6B *in vitro* and *in vivo*. We found lower expression of GPM6B in aggressive glioma. Receiver operating characteristic (ROC) analysis suggested that GPM6B is an indicator of mesenchymal subtype. Kaplan-Meier analysis also revealed that patients with glioma with high GPM6B expression levels had a tendency toward prolonged survival. The GPM6B expression level could predict favorable prognosis of patients independent of age, grade, IDH status, and 1p/19q status. Additionally, targeting GPM6B impaired the self-renewal and tumorgenicity of mesenchymal GSCs by inhibiting the activation of the Wnt pathway *in vitro* and *in vivo*. Our results demonstrated that GPM6B is a crucial predictor in glioma prognosis and represents an underlying therapeutic target in GSC therapy.

Keywords: GPM6B, molecular features, prognostic factor, glioblastoma stem cell, mesenchymal subtype

Introduction

As the most common primary malignant brain tumor in adults, according to the 2016 World Health Organization (WHO) classification, glioma can be diagnosed based on histopathology and molecular features [1, 2]. Despite the development of surgical, radio-, and chemotherapies, the current situation of glioma treatment remains unsatisfactory [3, 4]. Therefore, there is an urgent need to explore valid prognostic factors and therapeutic targets, to better understand the mechanism of glioma progression.

The important features of tumor development include angiogenesis and the decay of cell differentiation. A four-transmembrane protein, glycoprotein M6B (GPM6B), which belongs to the proteolipid protein (PLP) family, is widely expressed in neurons, oligodendrocytes, and astrocytes [5-7]. Previous studies have demonstrated that GPM6B plays a role in cell differentiation and neuronal myelination [8, 9]; thus, its role in tumors has been widely studied [10-12]. In intracranial tumors, the expression of GPM6B has been shown to distinguish glioblastoma multiforme and meningothelial meningioma in biopsies [13]. Given that glioma is the most common intracranial tumor, we attempted to investigate its functional role in this context.

Glioblastoma (GBM) is the most malignant glioma given its high invasion capability [14]. Glioblastoma stem cells (GSCs) are characterized by self-renewal and differentiation capacities, and have been implicated in tumor angiogenesis, invasion, and immune suppression, as

Table 1. Baseline characteristics of patients from the CGGA and TCGA cohorts

Variable		CGGA dataset	TCGA dataset
Age	< 45	191	267
	≥ 45	134	321
Sex	Male	203	343
	Female	122	245
Grade	II	103	212
	III	79	223
	IV	139	153
	NA	4	0
IDH1/2 status	Mutation	175	364
	Wild type	149	217
	NA	1	7
1p/19q status	Codeleted	67	146
	Non-Codeleted	250	437
	NA	8	5
Histological subtype	Classical	37	146
	Mesenchymal	81	30
	Neural	58	34
	Proneural	149	378

well as tumor initiation and progression [15, 16]. GBM and GBM-derived GSCs can be broadly classified into four major subtypes, namely classical, MES, neural, and proneural (PN). The clinical significance of MES GSCs is supported by their relative resistance to conventional chemotherapy and radiation compared to other subclasses [17]. Hence, understanding the regulation of MES GSCs is needed to improve the clinical outcome for patients with glioblastoma.

In this study, the clinical and molecular characteristics of GPM6B in glioma were emphasized and a favorable prognostic biomarker of glioma was found. External validation using a nomogram was performed with the Chinese Glioma Genome Atlas (CGGA) RNA sequencing data as the basic cohort, followed by verification in a dataset from The Cancer Genome Atlas (TCGA). Subsequently, Gene Ontology (GO) and Kyoto Encyclopedia of Genes and Genomes (KEGG) analyses were conducted to probe possible pathways. Overexpression of GPM6B suppressed the self-renewal and tumorgenicity of MES GSCs by inactivation of the Wnt pathway. Our study demonstrates the clinical and functional roles of GPM6B and suggests that targeting GPM6B may be effective in glioma.

Methods

Acquisition of data

All RNA sequencing data and clinical features of patients with glioma were downloaded from the CGGA dataset (n = 325) (http://www.cgga.org. cn) and TCGA dataset (n = 588) (http://cancergenome. nih.gov/). The patients' clinical and molecular information are described in **Table 1**.

Patients and samples

Glioma specimens were obtained from surgeries at the First Affiliated Hospital of Nanjing Medical University (**Table 2**). All of the enrolled patients signed the informed consent according to the institutional protocols (Ethics number: 2019-SR-479) by the Ethics Committee of the First Affiliated Hospital of Nanjing Medical University.

Survival analysis of GPM6B expression in glioma

Survival analysis was conducted to evaluate the prognostic value of GPM6B expression on overall survival (OS) in glioma. Statistical significance according to Kaplan-Meier survival curves was calculated using the log-rank test.

Development and validation of a nomogram

Univariate and multivariate Cox regressions, and a nomogram were employed and developed to determine other independent prognostic factors according to the methods outlined by our previous study [18]. The validation of nomogram-based prediction was conducted in both the CGGA and TCGA datasets.

Functional enrichment analysis

GO analysis was performed using the cluster profiler package, and the top 30 pathways and top 10 GO terms were visualized with R (Version 4.0.2). The KEGG (https://www.kegg.jp/kegg/) was used to reveal the important pathway associated with GPM6B, and the pathways with $P < 0.05$ were selected.

Quantitative RT-PCR

The total RNA was extracted from glioma cells using TRIzol reagent (Thermo Fisher Scientific, USA) following the manufacturer's instructions.

Table 2. Patient baseline characteristics from clinical samples

Sample ID	Sex	Age	Grade	Subtype
1	Male	65	WHO II	Non-Mesenchymal
2	Male	40	WHO II	Non-Mesenchymal
3	Female	54	WHO II	Non-Mesenchymal
4	Male	38	WHO III	Non-Mesenchymal
5	Female	54	WHO III	Non-Mesenchymal
6	Male	66	WHO III	Non-Mesenchymal
7	Female	55	WHO IV	Non-Mesenchymal
8	Male	56	WHO IV	Non-Mesenchymal
9	Female	57	WHO IV	Non-Mesenchymal
10	Male	58	WHO IV	Mesenchymal
11	Female	59	WHO IV	Mesenchymal
12	Male	60	WHO IV	Mesenchymal
13	Female	41	WHO IV	Non-Mesenchymal
14	Male	62	WHO IV	Non-Mesenchymal
15	Female	53	WHO IV	Non-Mesenchymal
16	Male	63	WHO II	Non-Mesenchymal
17	Female	44	WHO II	Non-Mesenchymal
18	Male	52	WHO III	Non-Mesenchymal
19	Female	51	WHO III	Non-Mesenchymal
20	Male	45	WHO IV	Mesenchymal

The Primer sequences were as follows: GPM6B forward: 5'-TCCTATCACCTGTTCATTGTGG-3' and reverse: 5'-GCAGCAATCTTCCCGACTC-3'. GAPDH forward: 5'-CCTTCTCCCCATTCCGTCTT-3' and reverse: 5'-AAATCAGGAGTGGGAGCACA-3'.

Western blot

After extraction, proteins in the cell lysates were first resolved by sodium dodecyl sulfate polyacrylamide gel electrophoresis (SDS-PAGE) and then transferred to nitrocellulose membrane. The membrane was subsequently blocked with 6% nonfat dry milk in TBST for 2 h before incubating with the following primary antibodies from Abcam: GPM6B (ab92-988, 1:250), CD44 (ab254530, 1:500), p-STAT3 (ab267373, 1:1000), STAT3 (ab68153, 1:1000), Wnt7b (ab94915, 1:500), β-catenin (ab16051, 1:3000), c-Myc (ab32072, 1:1000), and GAPDH (ab8245, 1:2000). After incubation with peroxidase-conjugated secondary antibodies, the signals were probed using the SuperSignal® Maximum Sensitivity Substrate (Thermo Fisher Scientific). The relative band intensity was analyzed using Image Lab software (Bio-Rad).

Immunohistochemistry (IHC)

Human glioma biopsy specimens were fixed with 4% paraformaldehyde, processed into 6-μm-thick sections and immune-stained with specific antibodies for GPM6B. The slides were imaged under a light microscope (Leica, Germany), and the percentage of positive cells was calculated by counting under high magnification (× 100).

Cell lines and reagents

GSC lines (MES: GSC28, GSC505) were established in a manner that has been widely applied in previous studies [19, 20]. GSCs were cultured in DMEM/F12 medium (10565018; Gibco, USA) supplemented with B27 (Invitrogen), basic Fibroblast Growth Factor (bFGF), and 20 ng/ml Epidermal Growth Factor (EGF) (236-EG; R&D Systems, USA), and incubated at 37°C with 5% CO_2. All cells were routinely proven to be free of mycoplasma.

Neurosphere formation assay

Dispersed single cells were plated at a density of 1 cell/μl and the spheres that formed after 1 to 2 weeks were examined. A microscope (Leica, Germany) was used to acquire images and quantification analysis was performed to measure the sphere diameters.

Extreme limiting dilution assay

Transfected GSCs were dissociated to single cells and then plated in 96-well plates at densities of 5, 10, 15, 20, 25, 30, 35, 40, 45, and 50 cells per well. Seven days after incubation, each well was examined for the formation of tumor spheres. The data were analyzed using Extreme Limiting Dilution Analysis (ELDA) software.

Vectors and lentiviral transfection

The overexpression plasmid vector of GSCs targeting GPM6B was purchased from Genepharma and validated by DNA sequencing.

Xenograft mouse model

The 6-week-old male nude mice used in this study were purchased from Nanjing Medical

University Animal Center. For intracranial xenograft experiments, GSCs lentivirally transduced with firefly luciferase (Fluc) were implanted into the frontal subdural region. The IVIS Imaging System (Caliper Life Sciences) was used to measure the intracranial tumor growth every 7 days. Each mouse was intraperitoneally injected with 150 μg/g D-luciferin (YEASEN, Shanghai, China) before imaging. The Living Images software package (Caliper Life Sciences) was applied to analyze the integrated flux of photons in each region. The procedures were approved by the Animal Management Rule of the Chinese Ministry of Health (documentation 55, 2001) and the Nanjing Medical University Animal Experimental Ethics Committee (Ethics number: IACUC-1907006).

Statistical analysis

Statistical analyses were performed using GraphPad Prism 8.0.2 software (GraphPad Software, USA) and R language for Windows, version 3.6.1 (http://www.r-project.org). Quantitative data were compared using a Student's *t*-test between two samples or one-way analysis of variance (ANOVA) for multiple samples. Statistical significance in Kaplan-Meier survival curves were calculated using the log-rank test. The subcutaneous tumor diameters in each group were analyzed using a two-way ANOVA. Cox regression analysis was performed using the survival package in R. All results are presented as the mean ± S.D. and repeated in at least three independent experiments. A p value < 0.05 was considered to indicate a significant difference.

Results

GPM6B expression was correlated with glioma grade, IDH mutation status, and glioma subtype

The flowchart of the study is presented in Supplementary Figure 1. The expression of GPM6B in gliomas was analyzed based on the WHO grade system, histopathology, and IDH mutation status. In the CGGA cohort, the expression of GPM6B was obviously decreased with the increase in grade (P < 0.0001) (**Figure 1A**). Similar results were obtained in TCGA cohort (P < 0.0001) (**Figure 1F**). According to the IDH status, patients with glioma were divided into two groups, namely the IDH mutation group and the IDH wild-type group, and the expression level of GPM6B was compared between them. In the CGGA cohort, the GPM6B expression in the IDH wild-type group was relatively lower than that in the IDH mutation group regardless of tumor grade (**Figure 1B**; Supplementary Figure 2A), which was also verified in the TCGA cohort (**Figure 1F**; Supplementary Figure 2B). These results suggested that GPM6B is negatively correlated with the malignancy of glioma. Next, to determine the relationship between GPM6B and glioma molecular subtypes, we investigated the expression of GPM6B between four TCGA subtypes. It was found that the mesenchymal subtype showed markedly decreased GPM6B expression compared to the other three subtypes in both the CGGA and TCGA cohorts (**Figure 1C**, **1G**). Subsequently, we calculated the receiver operating characteristic (ROC) curves of GPM6B expression and the mesenchymal subtype (**Figure 1D**, **1H**). In the CGGA cohort, the area under the curve (AUC) was 0.827 with an optimal cutoff value of 8.302 (the sensitivity and specificity were 0.736 and 0.795). In the TCGA cohort, the AUC was 0.806 with an optimal cutoff value of 14.225 (the sensitivity and specificity were 0.679 and 0.781). Thus, GPM6B may represent a biomarker to distinguish mesenchymal subtype and non-mesenchymal subtype in glioma.

Increased GPM6B expression predicted a better outcome

To further evaluate the prognostic value of GPM6B, patients with glioma were divided into $GPM6B^{low}$ and $GPM6B^{hi}$ groups based on a cutoff value (median GPM6B expression level). As shown in **Figure 2A** and **2D**, the $GPM6B^{low}$ group displayed a reduced overall survival time compared to their $GPM6B^{hi}$ counterparts in both the CGGA and TCGA datasets. Similar results were observed in patients with low-grade glioma (LGG) and GBM in Kaplan-Meier curves (**Figure 2B**, **2C**, **2E** and **2F**). Therefore, it was concluded that GPM6B could act as a favorable prognostic biomarker.

Construction and validation of a nomogram

Next, uni- and multivariate Cox regression analysis was performed to investigate the independent prognostic significance of GPM6B in the CGGA and TCGA datasets. Of note, although after adjusting for age, grade, IDH status and 1p/19q status, statistically meaningful prog-

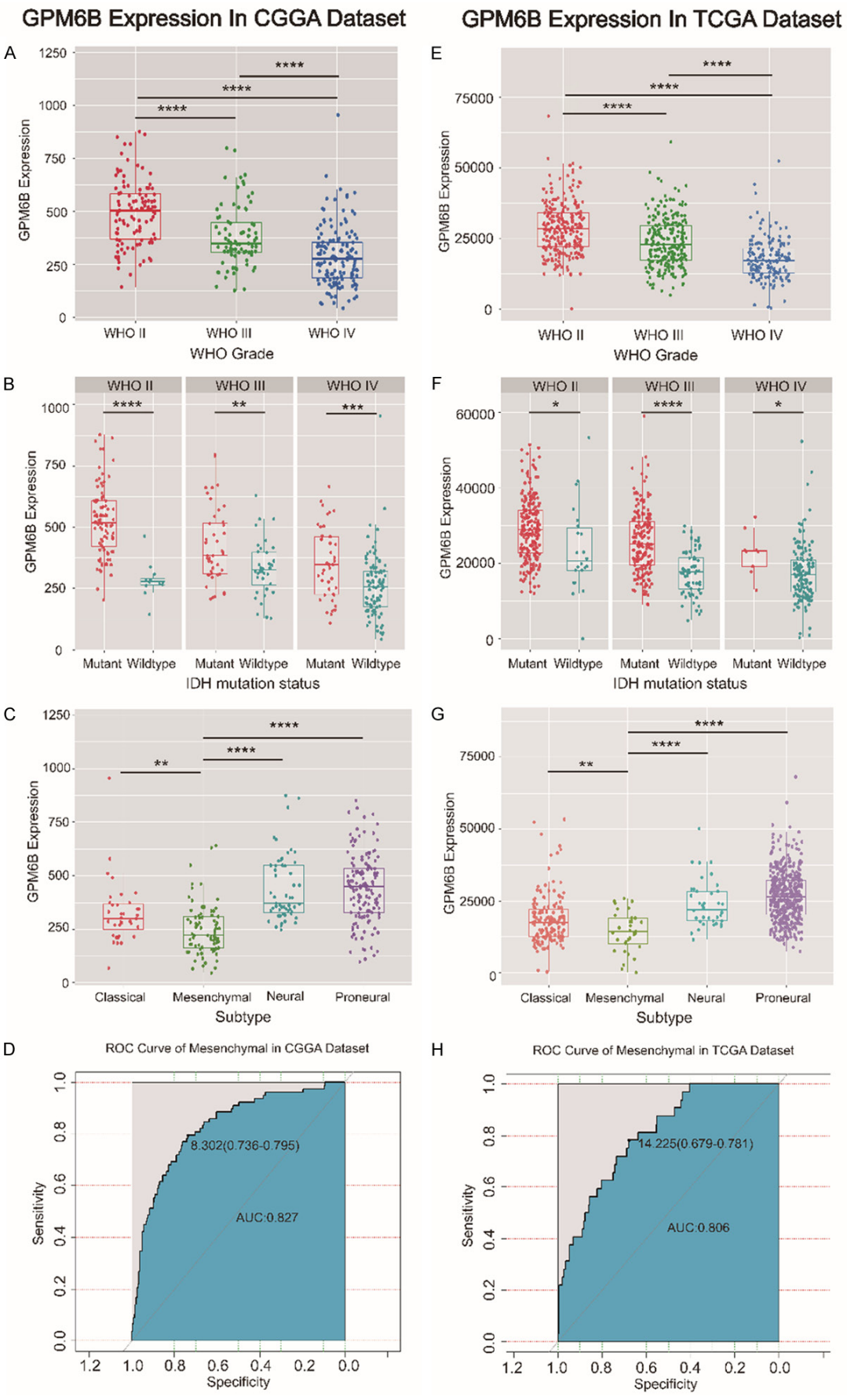
GPM6B Expression In CGGA Dataset
GPM6B Expression In TCGA Dataset
A
E
GPM6B Expression
WHO II
WHO III
WHO IV
WHO Grade
****
B
F
Mutant
Wildtype
IDH mutation status
*
**
***
C
G
Classical
Mesenchymal
Neural
Proneural
Subtype
D
H
ROC Curve of Mesenchymal in CGGA Dataset
ROC Curve of Mesenchymal in TCGA Dataset
Sensitivity
Specificity
8.302(0.736-0.795)
AUC:0.827
14.225(0.679-0.781)
AUC:0.806

Figure 1. Correlation between GPM6B expression and histologic/molecular subtypes. A-C, E-G. Comparison of the GPM6B expression level in the CGGA and TCGA cohorts according to WHO grade, IDH status, and TCGA molecular subtype. D, H. ROC curves for predicting mesenchymal subtype. *P < 0.05, **P < 0.01, ***P < 0.001.

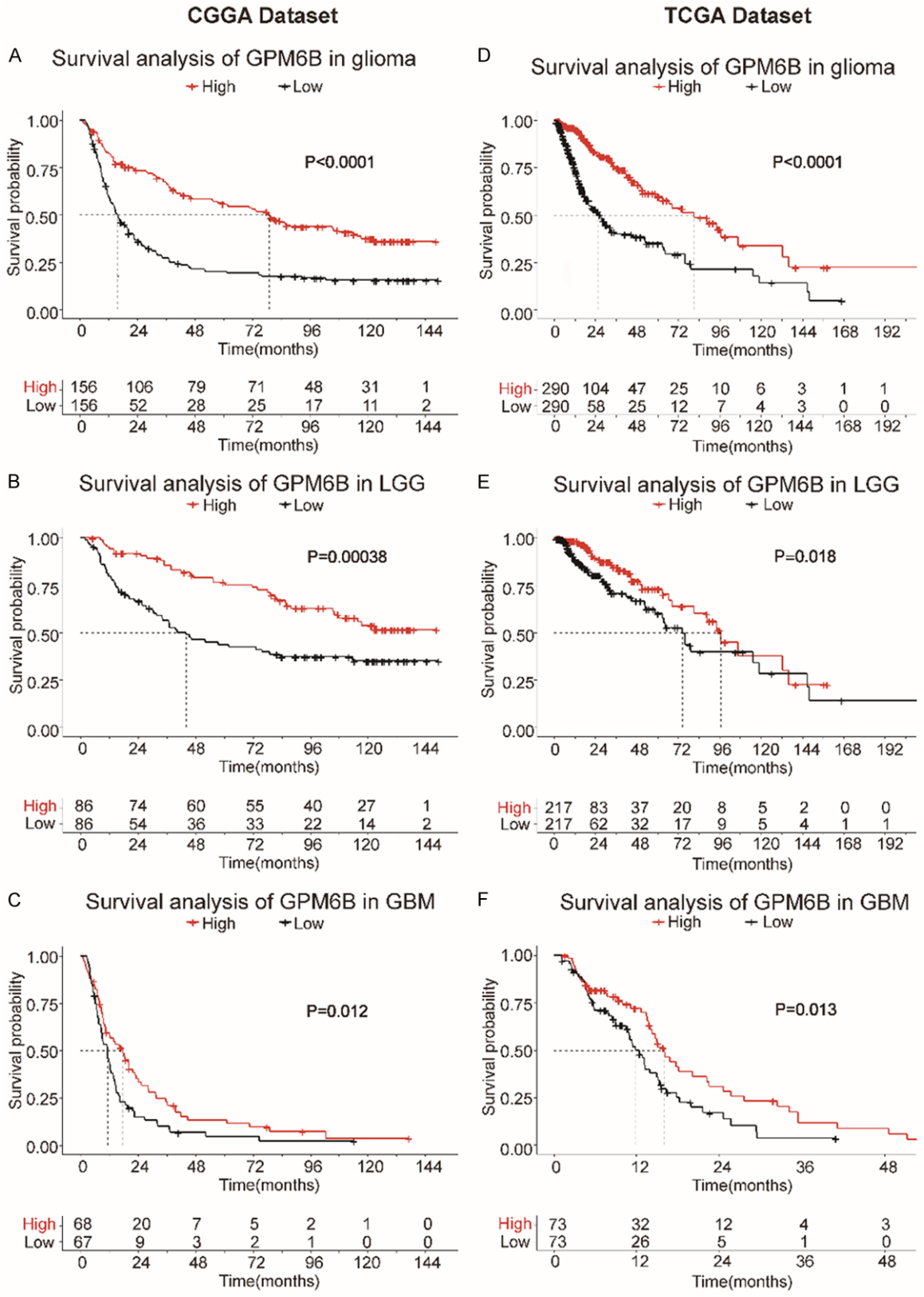

Figure 2. Survival differences in patients with glioma with high and low GPM6B expression status. A-F. Kaplan-Meier survival analysis of all grades glioma, LGG, and GBM in the CGGA and TCGA cohorts. *P < 0.05, **P < 0.01, ***P < 0.001.

nostic value was observed in the univariate analysis in the two datasets, GPM6B expression remained an independent prognostic factor for gliomas by multivariate Cox regression analysis (**Figure 3A**, **3B**). Furthermore, calibration illustrated sufficient prediction accuracy of the nomogram at 1-, 3-, and 5-year timepoints in the CGGA and TCGA (**Figure 3C-E**). A nomogram containing these independent factors was developed to forecast the survival probability of individuals (**Figure 3F**).

Potential functional analysis

To investigate the biologic behaviors of GPM6B, we calculated the genes that were significantly correlated with GPM6B (correlation R > 0.5 or R < -0.5) and differentiated into GPM6B^{low} and GPM6B^{hi} groups (log FC > 1) in the two datasets. Individually, 230 positively correlated genes and 42 negatively correlated genes in the TCGA cohort and 403 positively correlated genes and 473 negatively correlated genes in the CGGA cohort were identified (Supplementary Table 1). As shown, the negatively correlated genes of GPM6B were mainly focused on vascular development, cell adhesion, regulation of growth, multicellular organism development, and extracellular structure organization. However, the positively correlated genes mainly played vital functions in neuron/cell differentiation and morphogenesis, nervous system development, binding and metabolism of various hormones, cell junction, and integral to the membrane part. These findings suggest that the functional inquiry of GPM6B should be focused on cell differentiation.

Subsequently, GO analysis was performed with the R package, including biological process (BP), cellular composition (CC), and molecular function (MF) (**Figure 4A-D**; Supplementary Figure 2C, 2D). Among the BP section, axonogenesis, glial cell differentiation, and negative regulation of cell development are the most meaningful functions, which suggested that GPM6B plays a vital role in the biological genesis and development of gliomas. The results of the MF analysis displayed that actin binding was the major function of GPM6B in the treatment of glioma. Finally, in terms of KEGG analysis, the Wnt pathway, one of the main pathways associated with GSC identity [21], was highly related to the function of GPM6B (**Figure 4E**, **4F**).

GPM6B expression and phenotype were verified in vitro and in vivo

Consistent with the above results, the *in vitro* experiments with glioma samples using qRT-PCR (**Figure 5A**), WB (**Figure 5B**), and IHC (**Figure 5C**, **5D**) indicated that GPM6B expression was correlated with glioma grade and subtype.

Given the above results, the impact of GPM6B on mesenchymal identity in GSCs was investigated. Expectedly, the overexpression of GPM6B markedly attenuated cell growth and decreased tumorsphere formation ability (**Figure 6A**, **6B**), as revealed by the *in vitro* limiting dilution assay (**Figure 6C**). Furthermore, reduced expression of major MES-specific markers, including CD44 and phosphorylated STAT3 (p-STAT3), was observed in Lv-GPM6B MES GSCs compared to the vector (**Figure 6D**). Simultaneously, western blotting was performed to assess the expression of related genes within the Wnt signaling pathway in the GSC28 and GCS505 cell lines. It was found that GPM6B lessened the expression of Wnt7b, as well as β-catenin and c-Myc, which are downstream target genes (**Figure 6D**). These results suggested that GPM6B suppressed the identity of GSCs, at least in part, through inhibiting activation of the Wnt/β-catenin signaling pathway. Most importantly, in mouse orthotopic models, bioluminescent imaging revealed that the overexpression of GPM6B effectively inhibited the growth of GBM xenografts (**Figure 6E**).

Taken together, these results indicate that the overexpression of GPM6B inhibited the ability of self-renewal and tumorigenicity of MES GSCs through down-regulating the Wnt pathway, which may have a negative role in the maintenance of the MES subtype.

Discussion

Among the most aggressive and intractable tumors, primary brain tumors are the leading

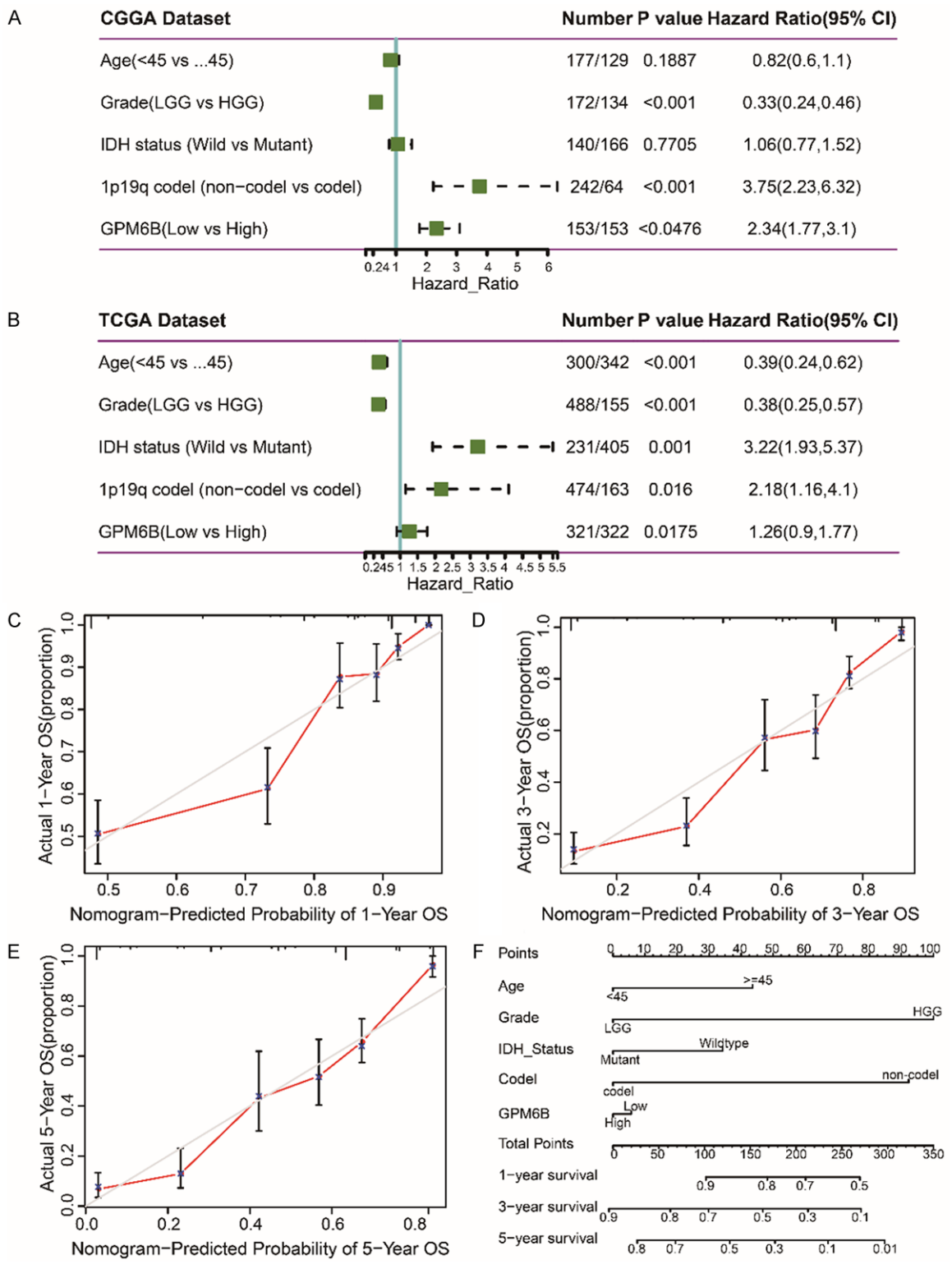

Figure 3. Development and validation of a nomogram. A, B. Forest plot of multi-variate Cox regression analysis on GPM6B and other factors. C-E. Calibration plot at 1, 3, and 5 years using the CGGA and TCGA datasets. F. Nomogram with independent prognostic factors.

cause of cancer in children younger than 15 years of age, and the second cause in adolescents older than 15 years of age [22, 23]. As the most aggressive and infiltrative of primary

A

CGGA Dataset

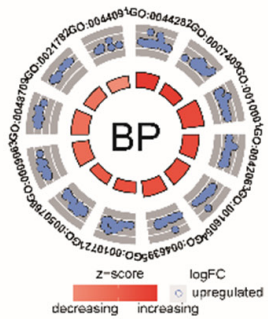

ID	Description
GO:0044282	small molecule catabolic process
GO:0007409	axonogenesis
GO:0010001	glial cell differentiation
GO:0042063	gliogenesis
GO:0016054	organic acid catabolic process
GO:0046395	carboxylic acid catabolic process
GO:0010721	negative regulation of cell development
GO:0050768	negative regulation of neurogenesis
GO:0009063	cellular amino acid catabolic process
GO:0048709	oligodendrocyte differentiation
GO:0021782	glial cell development
GO:0044091	membrane biogenesis

B

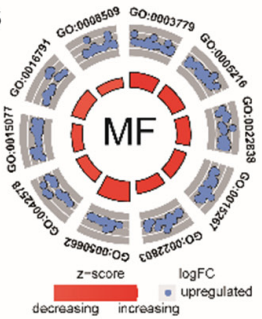

ID	Description
GO:0003779	actin binding
GO:0005216	ion channel activity
GO:0022838	substrate-specific channel activity
GO:0015267	channel activity
GO:0022803	passive transmembrane transporter activity
GO:0050662	coenzyme binding
GO:0042578	phosphoric ester hydrolase activity
GO:0015077	monovalent inorganic cation transmembrane transporter activity
GO:0016791	phosphatase activity
GO:0008509	anion transmembrane transporter activity

C

TCGA Dataset

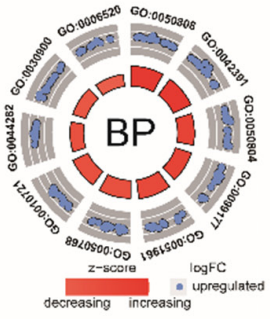

ID	Description
GO:0050808	synapse organization
GO:0042391	regulation of membrane potential
GO:0050804	modulation of chemical synaptic transmission
GO:0099177	regulation of trans-synaptic signaling
GO:0051961	negative regulation of nervous system development
GO:0050768	negative regulation of neurogenesis
GO:0010721	negative regulation of cell development
GO:0044282	small molecule catabolic process
GO:0030900	forebrain development
GO:0006520	cellular amino acid metabolic process

D

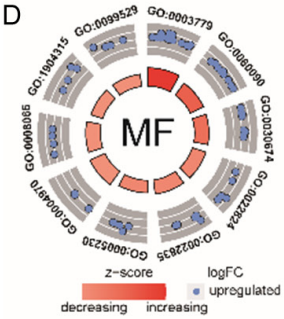

ID	Description
GO:0003779	actin binding
GO:0060090	molecular adaptor activity
GO:0030674	protein binding, bridging
GO:0022824	transmitter-gated ion channel activity
GO:0022835	transmitter-gated channel activity
GO:0005230	extracellular ligand-gated ion channel activity
GO:0004970	ionotropic glutamate receptor activity
GO:0008066	glutamate receptor activity
GO:1904315	channel activity involved in regulation of postsynaptic membrane potential
GO:0099529	activity involved in regulation of postsynaptic membrane potential

E

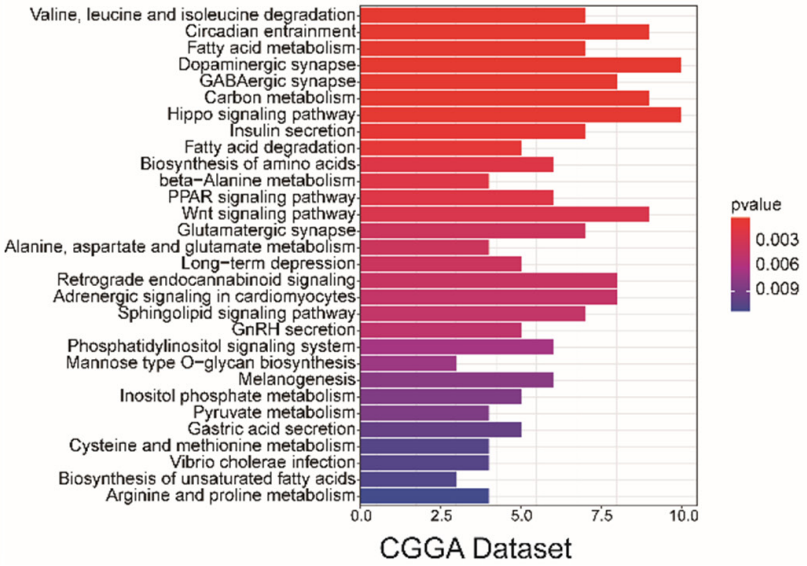

F

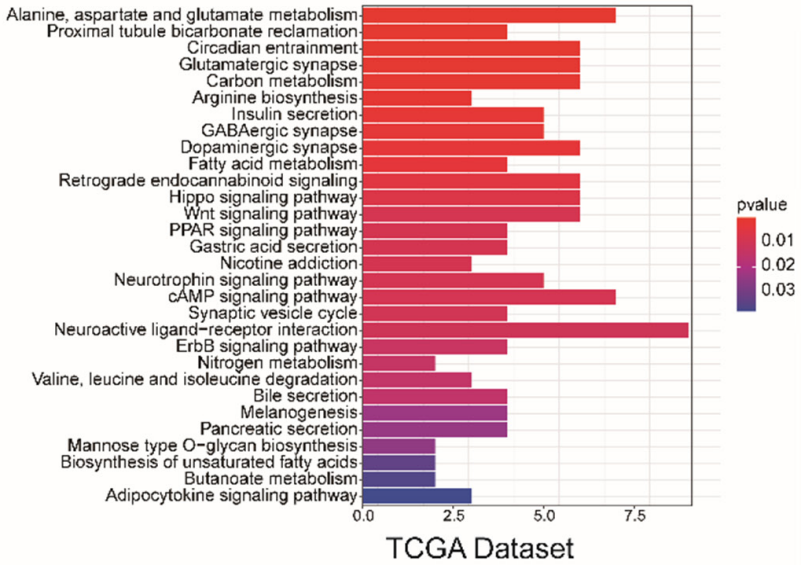

Figure 4. Pathway enrichment analysis. A-D. GO analysis for biological processes of GPM6B. E, F. KEGG pathways analysis of GPM6B.

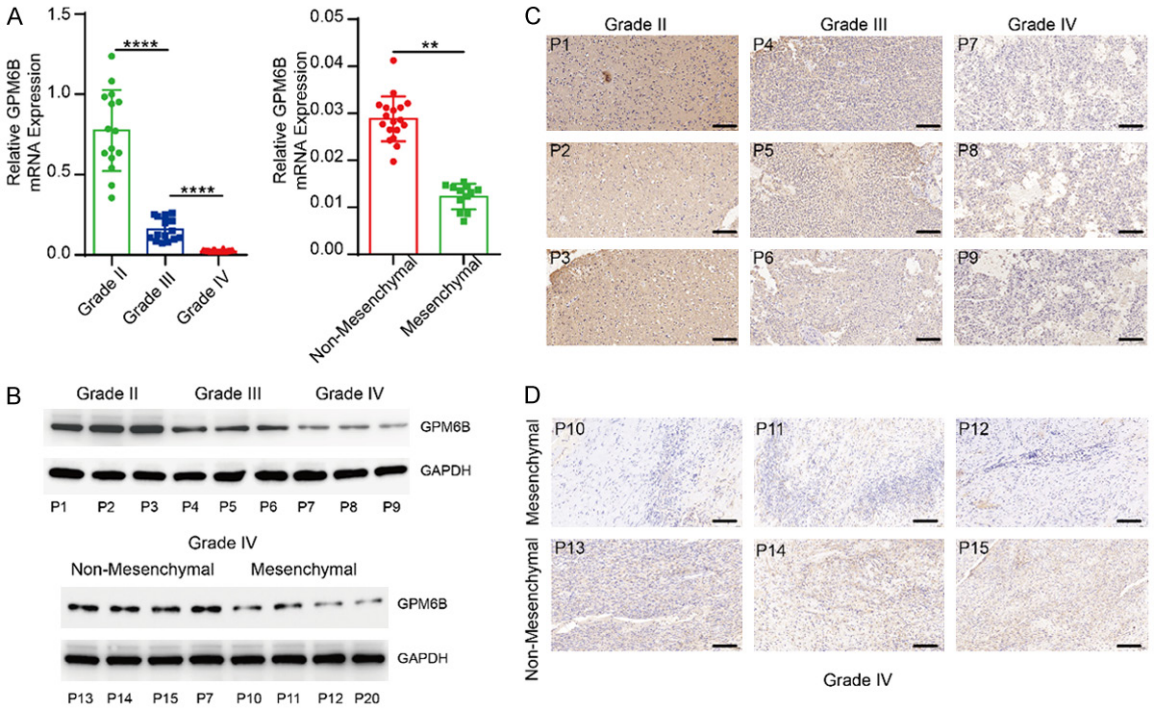

Figure 5. Validation of GPM6B expression *in vitro*. A. GPM6B mRNA expression in different grades of glioma and different subtypes was determined by qRT-PCR. Data are indicated as the mean ± S.D. B-D. GPM6B protein expression in different grades of glioma and different subtypes of GSCs was evaluated by western blot and IHC. GAPDH was used as control in western blot assays. Scale bar: 100 μm. *P < 0.05, **P < 0.01, ***P < 0.001. (n = 3 experiments).

brain tumors, gliomas have the highest mortality and a poor outcome [24]. Therefore, new diagnostic biomarkers and therapeutic approaches are urgently needed.

The PLP family plays a vital role in myelination and neuroprotection, especially in the central system, and is essential for cell differentiation and survival [25-28]. GPM6B is a member of the PLP family, which is found in a highly conserved gene sequence located at Xp22.2 [5, 6]. Thomson *et al.* reported that GPM6B mRNA was abundant in the perinatal central nervous system [6]. In functional experiments, GPM6B was firstly described as a brain-specific protein expressed mainly in neurons and oligodendrocytes; indeed, GPM6B is abundant in the brain and can discriminate glioma from meningioma [6, 7, 13]. Although the expression of GPM6B declines during development, it does remain into adulthood, suggesting that its function may be regulated intracellularly during CNS development. Researchers have suggested that GPM6B is localized at the cellular membrane of astrocytes and is involved in the regulation of neuroblast migration by participating in the modulation of transmembrane receptors related to downstream actin remodeling [29, 30]. In previous studies, Zhu *et al.* found that miR-1908-3p might promote proliferation and metastasis of breast cancer cells by suppressing GPM6B [10]. Moreover, Cyndia suggested GPM6B as an underlying new human lymphoid leukemia-associated oncogene [11]. He *et al.* demonstrated that GPM6B was a diagnostic marker of prostatic cancer (PCa) and contributed to the development of new treatment targets for PCa [12]. Nevertheless, the specific role and mechanism of GPM6B in gliomas has remained elusive.

In this study, the specific role and distribution of GPM6B in whole grade glioma were explored for the first time. CGGA and TCGA datasets

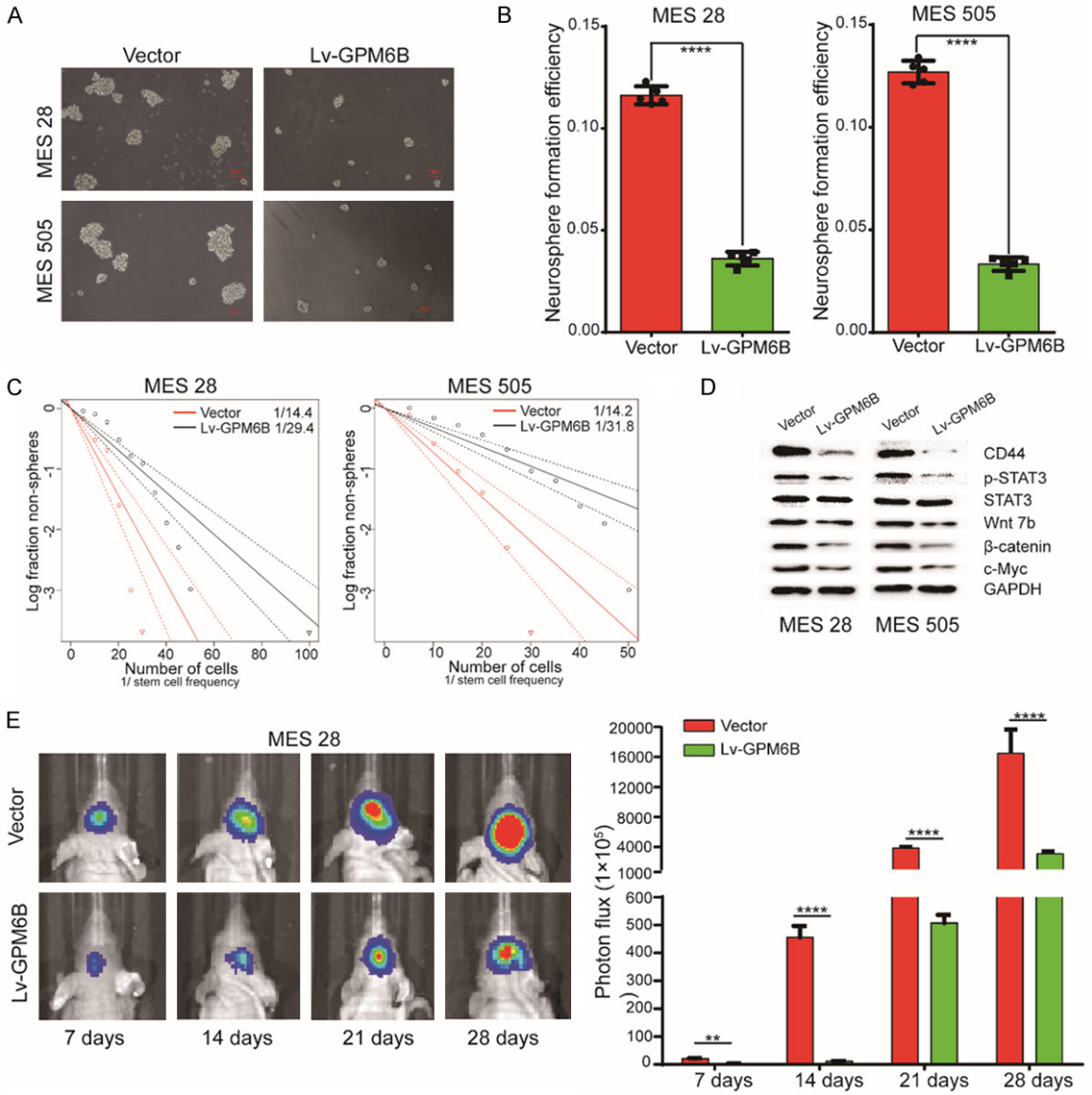

Figure 6. Overexpression of GPM6B impaired the self-renewal and tumorigenicity of MES GSCs *in vitro* and *in vivo*. A. Representative tumor sphere images of GSCs transfected with vector or Lv-GPM6B. Scale Bar: 100 μM. B. The data are indicated as the mean ± S.D. (n = 3). C. *In vitro* limiting dilution assay of MES 28 and 505 GSCs transduced with vector or Lv-GPM6B. D. Western blotting for CD44, p-STAT3, STAT3, Wnt7b, β-catenin, and c-Myc levels in MES 28 and 505 GSCs expressing vector or Lv-GPM6B. E. Bioluminescence imaging was performed on days 7, 14, 21, and 28 after implantation. *P < 0.05, **P < 0.01, ***P < 0.001.

were used to collect 913 samples for the analysis. The GPM6B expression level was found to be significantly down-regulated with the increase in grade. Furthermore, GPM6B expression was significantly decreased in glioma of the IDH wild-type group and may represent an underlying predicting marker for the mesenchymal subtype. These findings suggest that the GPM6B expression level is closely correlated with the malignant process in glioma. The risk of patients showing a lower GPM6B expression level in glioma development and progression was superior to those with higher GPM6B expression.

Additionally, the results of Kaplan-Meier survival curve analysis proved that higher GPM6B expression was correlated with a clear improvement in the overall survival of whole grade gliomas, LGG, and GBM. Besides, GPM6B was found to be an independent predictor of clinical prognosis by uni- and multivariate Cox regres-

sion analyses. These results further suggest that GPM6B is a pivotal composition for facilitating the benign development of glioma cells.

To further investigate the biologic function of GPM6B in glioma, R packages were used for GO analysis. The findings demonstrated that GPM6B was correlated with neuron/cell differentiation and morphogenesis, nervous system development, vascular development, cell adhesion, and the binding and metabolism of various hormones. These findings were consistent with GPM6B functions identified in other studies, such as the impact on neuron development, myelination, cell extension, and neuroblast migration as a result of GPM6B up-regulation [8, 9, 29, 31, 32]. Differentiation is essential for cell development, while dedifferentiation is central to cancer progression, including glioma [33, 34]. Therefore, restoring the differentiation function of tumor cells would be very useful for tumor therapy. GPM6B plays an important role in normal axonal extension and guidance *in vivo,* indicating that it is essential for neuron differentiation [31, 32]. Abnormal vascular development is another characteristic of tumor development [35], which was also revealed by the GO analysis for GPM6B. Moreover, KEGG analysis showed that Wnt/β-catenin signaling was highly relevant to GPM6B. A recent study illustrated that all of the included GSC subpopulations demonstrated increased Wnt/β-catenin signaling compared to the non-GSC components of the tumor, which suggested that the activation of this pathway is a common feature of GSCs [21]. Therefore, exploring the mechanism of GPM6B expression in glioma, especially in glioma cell differentiation and vascular development, may improve the survival of this fatal disease.

According to the diversity of the transcriptional, genotypic, and epigenetic states, GSCs are mainly classified into four subtypes [36]. Given that the mesenchymal (MES) subtype is generally associated with higher radio-resistance and is more prevalent in recurrent GBMs, targeting MES GSCs has become an indispensable consideration and an efficient therapeutic strategy for GBM. Prior studies have demonstrated that MES GSCs are associated with cancer development and progression by maintaining high activity, thus leading to poor prognosis compared to other GSCs [19, 37]. Here, it was identified that GPM6B could lead to the suppression of MES properties, including self-renewal, and tumorigenic capability of GSCs. Consistent with the pathway analysis, the relevant genes in the Wnt pathway were verified and down-regulated along with the increase in GPM6B. As a result, GPM6B may be developed as a novel target candidate for therapeutic intervention.

The clinical research of GPM6B in tumorigenesis is increasing recently. Since clinical data for utilizing GPM6B in human glioma are limited, more studies are urgently needed to reveal the function of GPM6B.

Conclusion

This study demonstrated that GPM6B is a favorable biomarker in glioma and an effective therapeutic target of MES GSCs. This study enhances the understanding of the mechanistic role of MES GSCs, suggesting that increased attention should be paid to the role of GPM6B in glioma treatment.

Acknowledgements

This study was funded by the National Natural Science Foundation of China (Grant No. 81972153), Jiangsu Province's Key Discipline of Medicine (Grant No. XK201117), and the Postgraduate Research & Practice Innovation Program of Jiangsu Province (SJCX20_0478).

Disclosure of conflict of interest

None.

Address correspondence to: Ning Liu, Department of Neurosurgery, The First Affiliated Hospital of Nanjing Medical University, 300 Guangzhou Road, Nanjing 210029, Jiangsu, China. Tel: +86-25-6830-3140; E-mail: liuning0853@126.com; Wei Tian, Department of Neurosurgery, Affiliated Hospital of Jiangnan University, Wuxi, Jiangsu, China. E-mail: a983314518@126.com

References

[1] Louis DN, Perry A, Reifenberger G, von Deimling A, Figarella-Branger D, Cavenee WK, Ohgaki H, Wiestler OD, Kleihues P and Ellison DW. The 2016 World Health Organization classification of tumors of the central nervous system: a summary. Acta Neuropathol 2016; 131: 803-820.

[2] Ostrom QT, Gittleman H, Liao P, Vecchione-Koval T, Wolinsky Y, Kruchko C and Barnholtz-Sloan JS. CBTRUS Statistical Report: primary brain and other central nervous system tumors diagnosed in the United States in 2010-2014. Neuro Oncol 2017; 19: v1-v88.

[3] Jiang T, Nam DH, Ram Z, Poon WS, Wang J, Boldbaatar D, Mao Y, Ma W, Mao Q, You Y, Jiang C, Yang X, Kang C, Qiu X, Li W, Li S, Chen L, Li X, Liu Z, Wang W, Bai H, Yao Y, Li S, Wu A, Sai K, Li G, Yao K, Wei X, Liu X, Zhang Z, Dai Y, Lv S, Wang L, Lin Z, Dong J, Xu G, Ma X, Zhang W, Zhang C, Chen B, You G, Wang Y, Wang Y, Bao Z, Yang P, Fan X, Liu X, Zhao Z, Wang Z, Li Y, Wang Z, Li G, Fang S, Li L, Liu Y, Liu S, Shan X, Liu Y, Chai R, Hu H, Chen J, Yan W, Cai J, Wang H, Chen L, Yang Y, Wang Y, Han L and Wang Q; Chinese Glioma Cooperative Group (CGCG); Society for Neuro-Oncology of China (SNO-China); Chinese Brain Cancer Association (CBCA); Chinese Glioma Genome Atlas (CGGA); Asian Glioma Genome Atlas (AGGA) network. Clinical practice guidelines for the management of adult diffuse gliomas. Cancer Lett 2016; 375: 263-273.

[4] Yang P, Wang Y, Peng X, You G, Zhang W, Yan W, Bao Z, Wang Y, Qiu X and Jiang T. Management and survival rates in patients with glioma in China (2004-2010): a retrospective study from a single-institution. J Neurooncol 2013; 113: 259-266.

[5] Olinsky S, Loop BT, DeKosky A, Ripepi B, Weng W, Cummins J, Wenger SL, Yan Y, Lagenaur C and Narayanan V. Chromosomal mapping of the human M6 genes. Genomics 1996; 33: 532-536.

[6] Vouyiouklis DA, Werner H, Griffiths IR, Stewart GJ, Armin-Nave K and Thomson CE. Molecular cloning and transfection studies of M6b-2, a novel splice variant of a member of the PLP-DM20/M6 gene family. J Neurosci Res 1998; 52: 633-640.

[7] Werner H, Dimou L, Klugmann M, Pfeiffer S and Nave KA. Multiple splice isoforms of proteolipid M6B in neurons and oligodendrocytes. Mol Cell Neurosci 2001; 18: 593-605.

[8] Zhang X, Xie H, Chang P, Zhao H, Xia Y, Zhang L, Guo X, Huang C, Yan F, Hu L, Lin C, Li Y, Xiong Z, Wang X, Li G, Deng L, Wang S and Tao L. Glycoprotein M6B interacts with TbetaRI to activate TGF-beta-Smad2/3 signaling and promote smooth muscle cell differentiation. Stem Cells 2019; 37: 190-201.

[9] Werner HB, Kramer-Albers EM, Strenzke N, Saher G, Tenzer S, Ohno-Iwashita Y, De Monasterio-Schrader P, Mobius W, Moser T, Griffiths IR and Nave KA. A critical role for the cholesterol-associated proteolipids PLP and M6B in myelination of the central nervous system. Glia 2013; 61: 567-586.

[10] Zhu Y, Wang Q, Xia Y, Xiong X, Weng S, Ni H, Ye Y, Chen L, Lin J, Chen Y, Niu H, Chen X and Lin Y. Evaluation of MiR-1908-3p as a novel serum biomarker for breast cancer and analysis its oncogenic function and target genes. BMC Cancer 2020; 20: 644.

[11] Charfi C, Edouard E and Rassart E. Identification of GPM6A and GPM6B as potential new human lymphoid leukemia-associated oncogenes. Cell Oncol (Dordr) 2014; 37: 179-191.

[12] He S, Huang Z, Li X, Ding Y, Sheng H, Liu B and Jia Z. GPM6B inhibit PCa proliferation by blocking prostate cancer cell serotonin absorptive capacity. Dis Markers 2020; 2020: 8810756.

[13] Castells X, García-Gómez JM, Navarro A, Acebes JJ, Godino O, Boluda S, Barceló A, Robles M, Ariño J and Arús C. Automated brain tumor biopsy prediction using single-labeling cDNA microarrays-based gene expression profiling. Diagn Mol Pathol 2009; 18: 206-218.

[14] Weller M, Wick W, Aldape K, Brada M, Berger M, Pfister SM, Nishikawa R, Rosenthal M, Wen PY, Stupp R and Reifenberger G. Glioma. Nat Rev Dis Primers 2015; 1: 15017.

[15] Cheng L, Huang Z, Zhou W, Wu Q, Donnola S, Liu JK, Fang X, Sloan AE, Mao Y, Lathia JD, Min W, McLendon RE, Rich JN and Bao S. Glioblastoma stem cells generate vascular pericytes to support vessel function and tumor growth. Cell 2013; 153: 139-152.

[16] Bao S, Wu Q, Sathornsumetee S, Hao Y, Li Z, Hjelmeland AB, Shi Q, McLendon RE, Bigner DD and Rich JN. Stem cell-like glioma cells promote tumor angiogenesis through vascular endothelial growth factor. Cancer Res 2006; 66: 7843-7848.

[17] Bao S, Wu Q, McLendon RE, Hao Y, Shi Q, Hjelmeland AB, Dewhirst MW, Bigner DD and Rich JN. Glioma stem cells promote radioresistance by preferential activation of the DNA damage response. Nature 2006; 444: 756-760.

[18] Qiu H, Tian W, He Y, Li J, He C, Li Y, Liu N and Li J. Integrated analysis reveals prognostic value and immune correlates of CD86 expression in lower grade glioma. Front Oncol 2021; 11: 654350.

[19] Chen Z, Wang HW, Wang S, Fan L, Feng S, Cai X, Peng C, Wu X, Lu J, Chen D, Chen Y, Wu W, Lu D, Liu N, You Y and Wang H. USP9X deubiquitinates ALDH1A3 and maintains mesenchymal identity in glioblastoma stem cells. J Clin Invest 2019; 129: 2043-2055.

[20] Guda MR, Labak CM, Omar SI, Asuthkar S, Airala S, Tuszynski J, Tsung AJ and Velpula KK. GLUT1 and TUBB4 in glioblastoma could be efficacious targets. Cancers (Basel) 2019; 11: 1308.

[21] Galdieri L, Jash A, Malkova O, Mao DD, DeSouza P, Chu YE, Salter A, Campian JL, Naegle KM,

Brennan CW, Wakimoto H, Oh ST, Kim AH and Chheda MG. Defining phenotypic and functional heterogeneity of glioblastoma stem cells by mass cytometry. JCI Insight 2021; 6: e128456.
[22] Oliver TG and Wechsler-Reya RJ. Getting at the root and stem of brain tumors. Neuron 2004; 42: 885-888.
[23] Baldwin RT and Preston-Martin S. Epidemiology of brain tumors in childhood - a review. Toxicol Appl Pharmacol 2004; 199: 118-131.
[24] Behin A, Hoang-Xuan K, Carpentier AF and Delattre JY. Primary brain tumours in adults. Lancet 2003; 361: 323-331.
[25] Brown FR 3rd, Beck JC, Niebyl JR and Singh I. Effect of proteolipid protein on central nervous system myelin membrane fluidity. Neurosci Lett 1985; 59: 149-154.
[26] Mobius W, Patzig J, Nave KA and Werner HB. Phylogeny of proteolipid proteins: divergence, constraints, and the evolution of novel functions in myelination and neuroprotection. Neuron Glia Biol 2008; 4: 111-127.
[27] Sapirstein VS, Nolan C, Stern R, Ciocci M and Masur SK. Identification of the plasma membrane proteolipid protein as a constituent of brain coated vesicles and synaptic plasma membrane. J Neurochem 1988; 51: 925-933.
[28] Fernandez ME, Alfonso J, Brocco MA and Frasch AC. Conserved cellular function and stress-mediated regulation among members of the proteolipid protein family. J Neurosci Res 2010; 88: 1298-1308.
[29] Choi KM, Kim JY and Kim Y. Distribution of the immunoreactivity for glycoprotein M6B in the neurogenic niche and reactive glia in the injury penumbra following traumatic brain injury in mice. Exp Neurobiol 2013; 22: 277-282.
[30] Fjorback AW, Muller HK and Wiborg O. Membrane glycoprotein M6B interacts with the human serotonin transporter. J Mol Neurosci 2009; 37: 191-200.
[31] Bang ML, Vainshtein A, Yang HJ, Eshed-Eisenbach Y, Devaux J, Werner HB and Peles E. Glial M6B stabilizes the axonal membrane at peripheral nodes of Ranvier. Glia 2018; 66: 801-812.
[32] Mita S, de Monasterio-Schrader P, Funfschilling U, Kawasaki T, Mizuno H, Iwasato T, Nave KA, Werner HB and Hirata T. Transcallosal projections require glycoprotein M6-dependent neurite growth and guidance. Cereb Cortex 2015; 25: 4111-4125.
[33] Biava PM, Burigana F, Germano R, Kurian P, Verzegnassi C and Vitiello G. Stem cell differentiation stage factors and their role in triggering symmetry breaking processes during cancer development: a quantum field theory model for reprogramming cancer cells to healthy phenotypes. Curr Med Chem 2019; 26: 988-1001.
[34] Friedmann-Morvinski D, Bushong EA, Ke E, Soda Y, Marumoto T, Singer O, Ellisman MH and Verma IM. Dedifferentiation of neurons and astrocytes by oncogenes can induce gliomas in mice. Science 2012; 338: 1080-1084.
[35] Folkman J. Role of angiogenesis in tumor growth and metastasis. Semin Oncol 2002; 29: 15-18.
[36] Patel AP, Tirosh I, Trombetta JJ, Shalek AK, Gillespie SM, Wakimoto H, Cahill DP, Nahed BV, Curry WT, Martuza RL, Louis DN, Rozenblatt-Rosen O, Suva ML, Regev A and Bernstein BE. Single-cell RNA-seq highlights intratumoral heterogeneity in primary glioblastoma. Science 2014; 344: 1396-1401.
[37] Chen Z, Wang H, Zhang Z, Xu J, Qi Y, Xue H, Gao Z, Zhao R, Wang S, Zhang S, Qiu W, Guo X and Li G. Cell surface GRP78 regulates BACE2 via lysosome-dependent manner to maintain mesenchymal phenotype of glioma stem cells. J Exp Clin Cancer Res 2021; 40: 20.

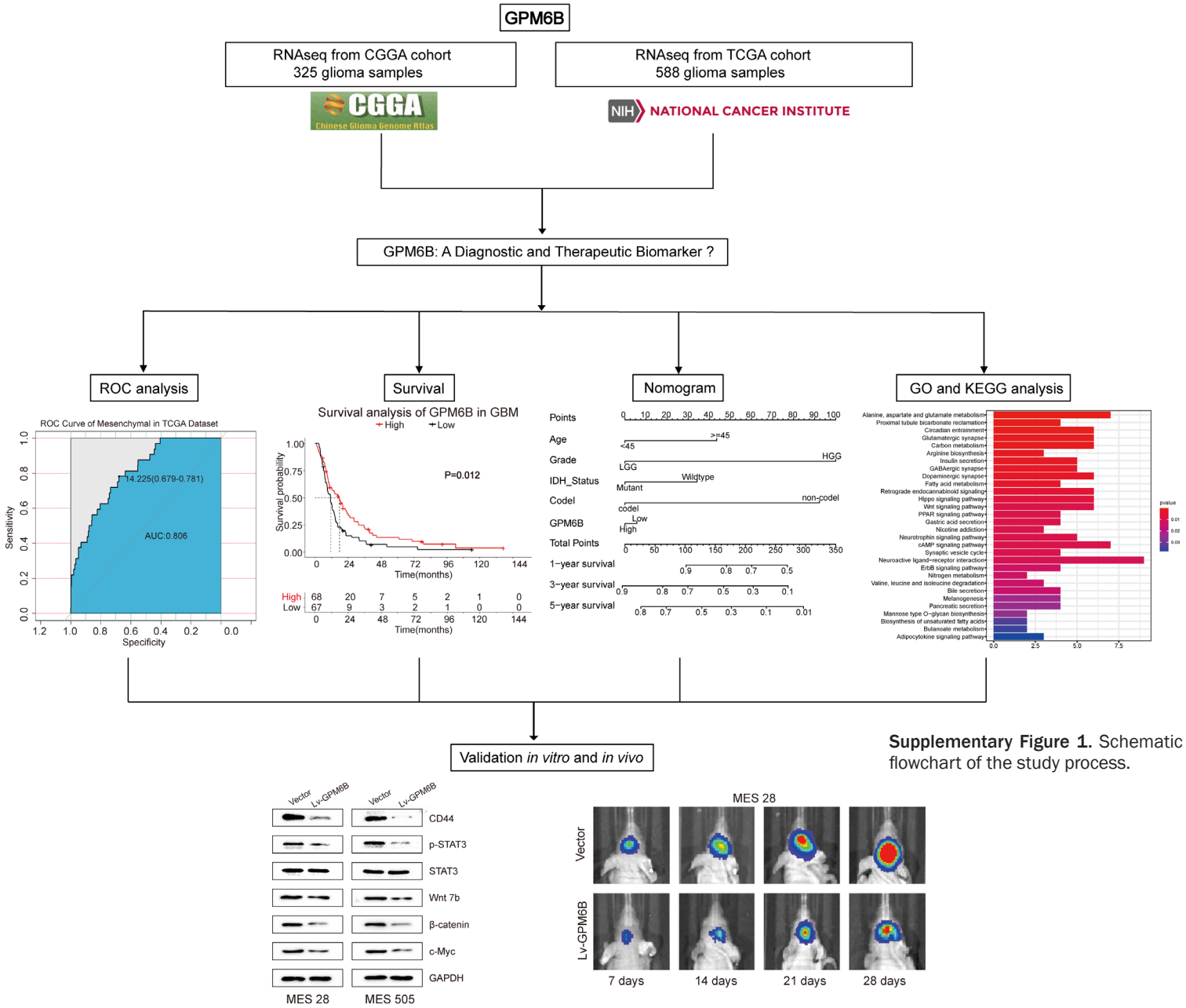

Supplementary Figure 1. Schematic flowchart of the study process.

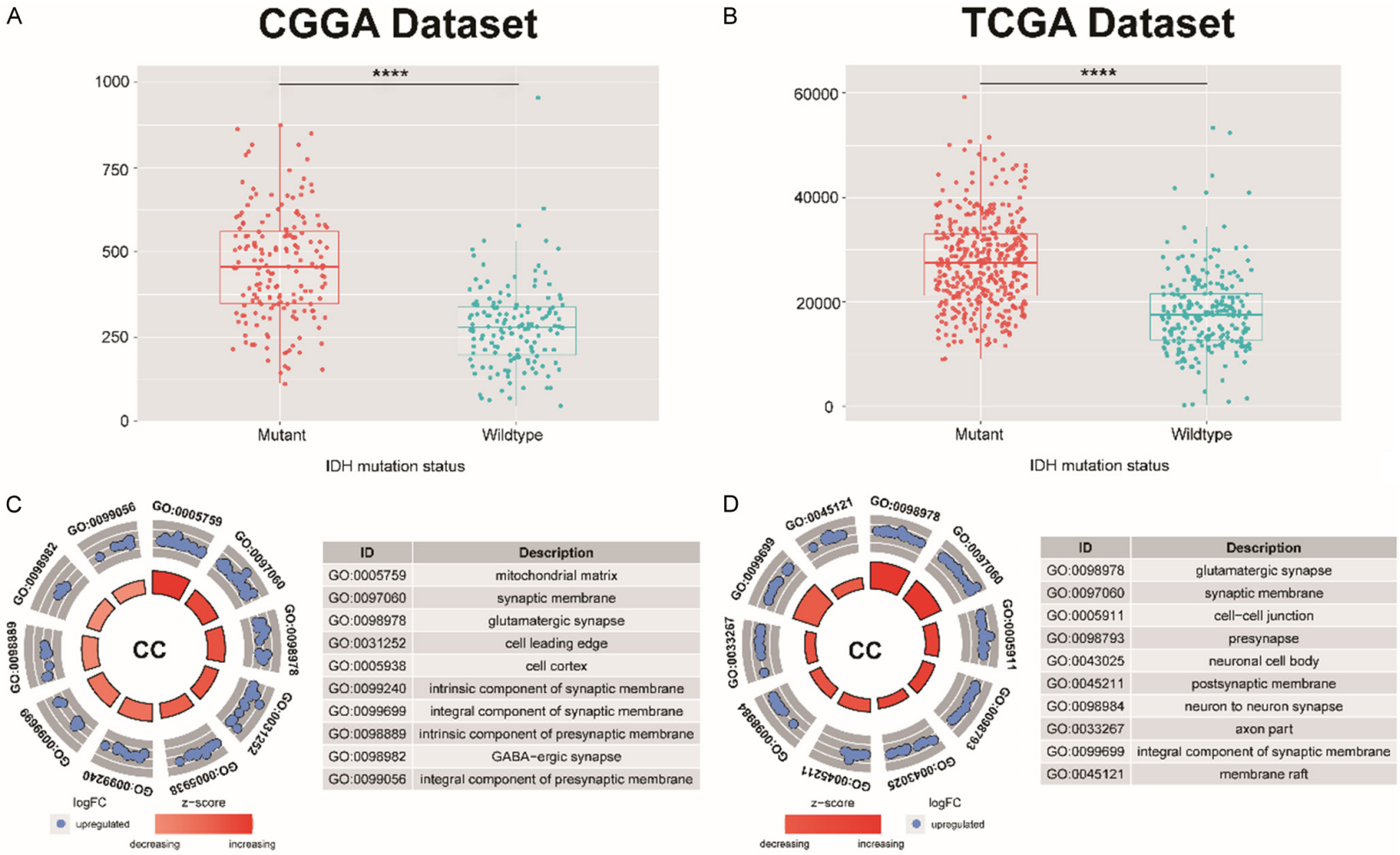

ID	Description
GO:0005759	mitochondrial matrix
GO:0097060	synaptic membrane
GO:0098978	glutamatergic synapse
GO:0031252	cell leading edge
GO:0005938	cell cortex
GO:0099240	intrinsic component of synaptic membrane
GO:0099699	integral component of synaptic membrane
GO:0098889	intrinsic component of presynaptic membrane
GO:0098982	GABA-ergic synapse
GO:0099056	integral component of presynaptic membrane

ID	Description
GO:0098978	glutamatergic synapse
GO:0097060	synaptic membrane
GO:0005911	cell-cell junction
GO:0098793	presynapse
GO:0043025	neuronal cell body
GO:0045211	postsynaptic membrane
GO:0098984	neuron to neuron synapse
GO:0033267	axon part
GO:0099699	integral component of synaptic membrane
GO:0045121	membrane raft

Supplementary Figure 2. A, B. Comparison of GPM6B expression level in the CGGA and TCGA cohorts with different IDH status. C, D. GO analysis for biologic processes of GPM6B.